Hindawi Publishing Corporation
International Journal of Optics
Volume 2012, Article ID 132542, 5 pages
doi:10.1155/2012/132542

Research Article

Ultrafast Plasmonic Nanoantenna-ITO Hybrid Switches

Martina Abb and Otto L. Muskens

SEPnet and the Department of Physics and Astronomy, University of Southampton, Highfield, Southampton SO17 1BJ, UK

Correspondence should be addressed to Otto L. Muskens, o.muskens@soton.ac.uk

Received 31 August 2011; Revised 13 October 2011; Accepted 14 October 2011

Academic Editor: Alexandre Bouhelier

We present here a new type of device using nonlinear hybrid antenna-semiconductor (ITO) interaction. We observe a picosecond transient response from the antenna that cannot be explained by either pure ITO or antenna nonlinearities independently. We study the dependence of the hybrid interaction on several experimental parameters, including the polarization of excitation and detection.

Nanoscale plasmonic components such as nanoantennas [1, 2] are of enormous interest for their capabilities of locally enhancing electromagnetic fields and controlling emission. Active control of such components will enable a new generation of tunable devices. We recently introduced a new concept of antenna switches relying on photoconductive loading of the gap between the arms of a dimer antenna [3]. Experimentally, modulation of localized plasmon modes has been achieved using the refractive index of liquid crystals [4]. Active tuning of the antenna gap has also been demonstrated using mechanical means, such as using stretchable elastomeric films [5] to reversibly engineer the distance between particle dimers. The temporal response of these changes is limited by the gap loading mechanisms that are used.

As a potentially ultrafast implementation of our concept [3], we demonstrated experimentally picosecond all-optical control of a plasmonic nanoantenna on ITO, referred to as an nanoantenna-ITO hybrid [6]. For ITO, unity-order changes of the refractive index have been achieved [7] by applying an electric field. We have shown that optical pumping of ITO leads to a local reduction of the free-carrier density in the substrate. The transient nonlinear response of the antenna-ITO hybrid shows a redshift of the plasmon resonance, as opposed to transient bleaching on SiO_2.

Here, we present a detailed study of the response of antennas on 20 nm thick ITO film (low cond.), both with and without ITO cover layer. We find an effect for both perpendicular and parallel modes of the antenna, although the parallel mode shift is more pronounced, as well as a polarization dependence of the pump beam. Additionally, we look at the interaction of a larger cylindrical goldpad with the ITO surrounding it to further investigate the injection mechanism of fast electrons from the gold into the ITO.

Nanoantennas were fabricated with e-beam lithography on low-conductivity (70–100 Ω/sq, 20 nm thick) and high-conductivity (8–12 Ω/sq, 120 nm thick) ITO substrates from Sigma-Aldrich using a bilayer of photoresist. After exposure and development, 25 nm of gold was deposited, followed by liftoff. To stay in focus when moving away from the edge of the sample, pads were burned along the way, which turned out useful as a test area later. The nanostructures were covered by sputtering a matching ITO layer of 25 nm on either top or left without cover. This did not produce a measurable difference, as we shall see.

For ultrafast spectroscopy, pulses of 4 ps length with a repetition rate of 40 MHz from an ytterbium fiber laser amplifier (Fianium, Ltd.) were used. The linear antenna response was spectrally characterized using the spatial modulation technique [8, 9], selecting wavelengths between 500–1800 nm using a subtractive mode double prism monochromator. The tunable probe beam was focused onto the sample from the front with a Mitutoyo 100x NIR objective with 0.5 NA, giving a spot size of 0.7 μm FWHM for 900 nm wavelength. As pump beam, we split off part of the original 1064 nm beam and frequency-double it with a 5 mm KTP

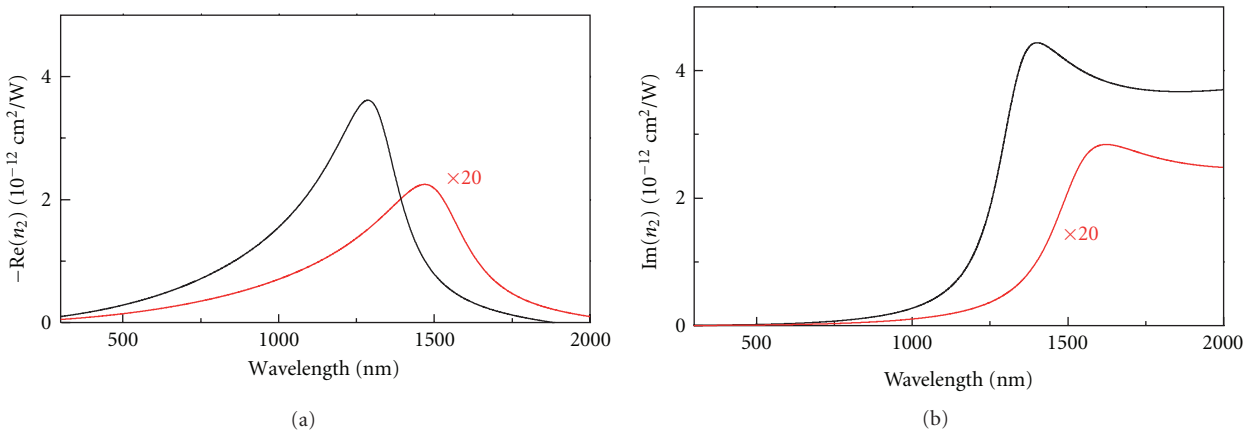

Figure 1: Free-carrier nonlinearity described by the nonlinear coefficient for 20 nm low-conductivity (red) and 120 nm high-conductivity (black) ITO.

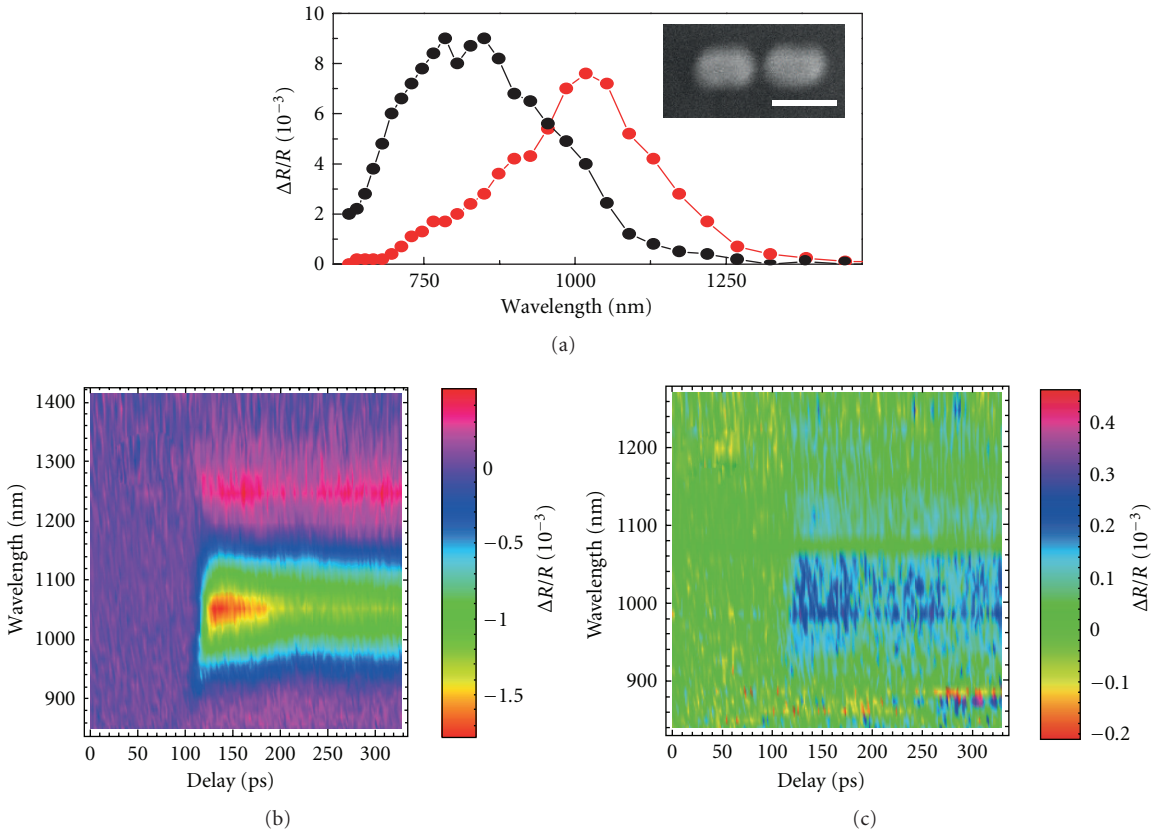

Figure 2: (a) Plasmonic resonances along the long (red circles) and the short (black circles) axis of our dimer antenna on low-conductivity ITO, covered with a 20 nm layer of low-conductivity ITO. The inset shows a SEM picture of the antenna, with the scale bar being for 200 nm. (b) and (c) depict the time traces of the pump probe nonlinear response, (b) for the longitudinal and (c) for the transversal mode.

crystal to obtain a 532 nm beam which was focused on the backside of the sample by a 0.6 NA aspheric lens, yielding a spot of 2 μm FWHM. To characterize the nonlinearity of the ITO and the antenna-ITO hybrids, we took time-resolved scans for different wavelengths to give a clear picture of the dynamics.

The nonlinearity of ITO is governed by the free-carrier density, as shown in [6]. This third-order nonlinearity can be expressed by a nonlinear coefficient n_2, representing the resulting refractive index modulation normalized to the optical peak intensity of the excitation beam: $n_2 = \Delta n/I$.

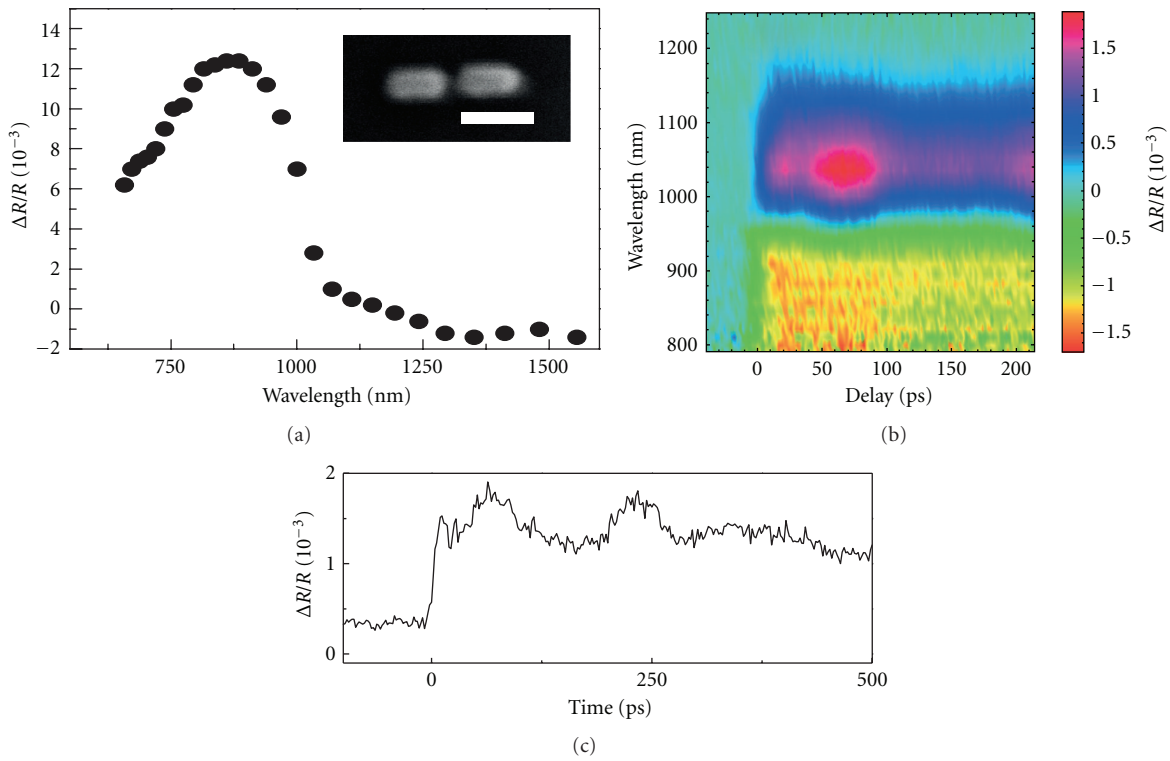

FIGURE 3: Spectral resonance of an antenna with a gap of 40 nm on low-conductivity ITO without cover. Optical pumping leads to a redshift of the original resonance. To the left of the plasmonic resonance and on the maximum of the pump probe signal, we observe an acoustic mode.

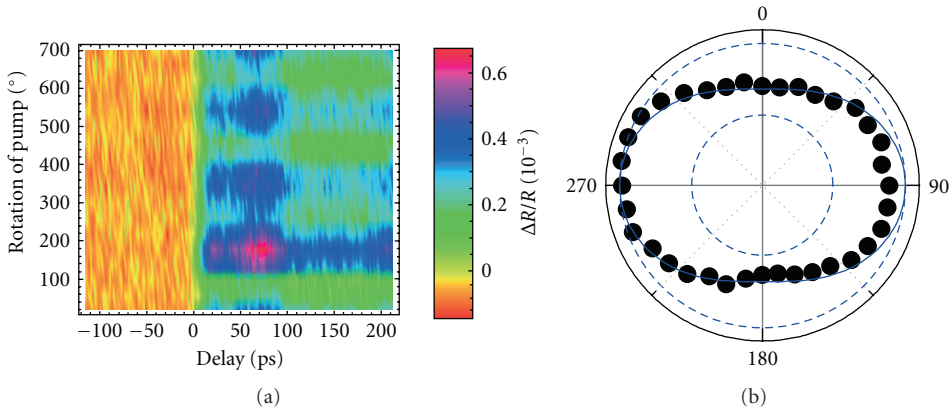

FIGURE 4: Dependence of the pump probe signal from Figure 3 on the polarization of the pump.

Resulting values of n_2 for both the real and the imaginary part of this nonlinear refractive index coefficient over the spectral range are shown in Figure 1 for 20 nm of low-conductivity and 120 nm of high-conductivity ITO. These are obtained from fits to the experimental reflectivity data shown in [6], where we found initial carrier concentrations of $N = 9.2 \times 10^{20}\,\mathrm{cm}^{-3}$ for the high-conductivity ITO and $N = 7.3 \times 10^{20}\,\mathrm{cm}^{-3}$ for the low-conductivity ITO. Optical pumping with 532 nm and 180 pJ pump energy was shown to deplete the ITO, and we observed changes in carrier concentration of $\Delta N = (2.1 \pm 0.1) \times 10^{18}\,\mathrm{cm}^{-3}$ for the high-conductivity ITO and $\Delta N = (5.4 \pm 0.2) \times 10^{16}\,\mathrm{cm}^{-3}$ for the low-conductivity ITO. We find a much larger nonlinearity (more than a factor 20) for the high-conductivity ITO, as can be expected. Our values for the Kerr nonlinearity are in excellent agreement with literature values of similar ITO films [10], taken at a single wavelength around 720 nm.

On the antennas, we measure the extinction spectra of an antenna with a gap of 40 nm on low-conductivity ITO, covered with a matching layer of ITO. We find a resonance at around 800 nm for the perpendicular mode

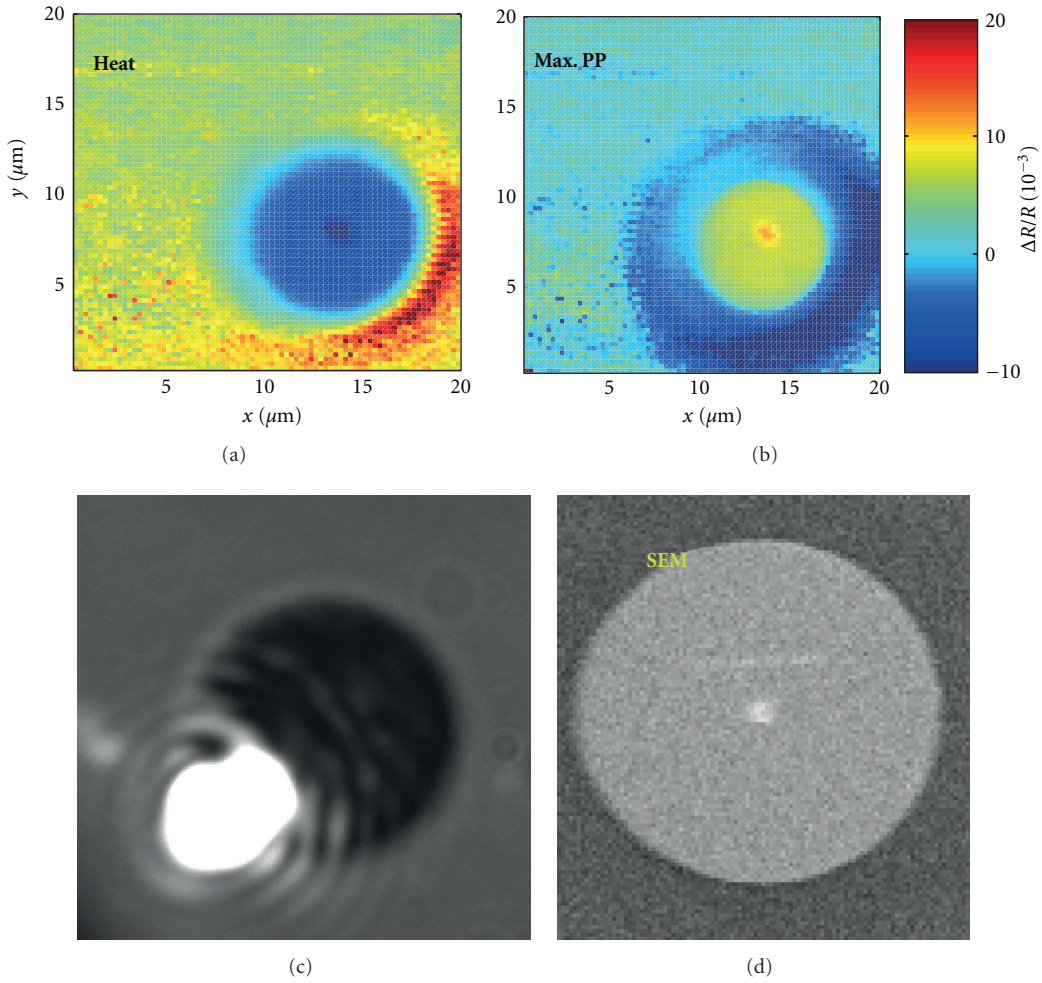

Figure 5: Pump probe signal around a gold pad at 985 nm probe wavelength and a pump energy of 180 pJ, for the heat background (a) and the maximum pump probe signal with the heat background subtracted (b). Below are a microscope image with the beam on the edge of the contamination dot (c) and a SEM image of the dot (d).

and another at around 1000 nm for the parallel antenna mode, see Figure 2(a). The corresponding that spectrally resolved nonlinear time trace is shown in Figures 2(b) and 2(c), with the heat backround already subtracted. The spectral bipolar form is different from the well-known transient bleaching found for all kinds of nanoparticles [11, 12], which corresponds to a decrease and broadening of the plasmonic resonance due to fast electron generation in the particle which leads to a change in the refractive index of the gold itself. Instead, we observe a bipolar transient response for both polarizations, although the effect is more pronounced for polarization parallel to the antenna. The negative pump probe signal can be identified with the spatial modulation extinction spectra, with a new redshifted resonance appearing next to it.

When modelling single antenna extinction spectra with FEM simulations (Comsol v3.5), the refractive index change and the concomitant resonance shift predicted for changes in carrier density of the order of our measured value for just the ITO film, $\Delta N = (2.1 \pm 0.1) \times 10^{18}\,\mathrm{cm}^{-3}$ cannot account for the large shift. This leads us to deduce that this must be an effect of the hybrid ITO-antenna system, as described in [6]. We propose that the shift is caused by hot electron injection from the gold into the surrounding ITO. This proposed energy transfer mechanism consists of two parts: first, hot electrons are injected from the antennas into the ITO substrate, leading to a temperature increase in the close vicinity. Apart from the heating effect, the hot electrons are not accountable for changes in the refractive index, since they are swiftly replaced by cold electrons transferring back to the antenna. But the heating effect is big enough to give way to a secondary effect, that of migration of free carriers from the heated region to the surrounding ITO, thus effectively depleting the ITO. This depletion changes the local refractive index of the ITO and therefore shifts the plasmon resonance of the antenna. The nonlinear coefficients needed to describe the Kerr ITO-antenna hybrid nonlinearity is a factor 37 larger than the pure substrate in the case of high-conductivity ITO and as large as a factor of 1475

in the case of low-conductivity ITO (see [6]), which makes the results for low-conductivity ITO-antenna hybrids even more remarkable.

Another notable difference between antennas on low- and high-conductivity ITO that supports our proposition is the fact that we observe acoustic modes in the fast nonlinear response of hybrids on low-conductivity ITO, as shown in Figure 3, but not for hybrids on high-conductivity ITO [6]. This was the case for 11 out of 17 antennas on low-conductivity ITO, for 15 out of 24 antennas on SiO_2, and for none of the 19 antennas on high-conductivity ITO that we have studied. These vibrations are present only on the maximum signal of the new redshifted mode and have oscillation periods of 100–300 ps for our antennas, depending on size. The reason for this position of the acoustic modes is still unclear. Their occurrence, however, indicates that the fast electrons that are excited by the pump beam transfer their energy to the lattice which starts the vibrations in the nanostructure. On high-conductivity ITO, on the other hand, we did not observe these lattice vibrations [6], which leads us to believe that the energy is not transferred to the lattice, but instead is dissipated into heat after the hot electrons are injected into the surrounding semiconductor.

In Figure 4, we show measurements of the excitation anisotropy for an antenna on low-conductivity ITO obtained by rotating a half-wave plate in the pump beam. We find an excitation anisotropy $(\Delta R_{\parallel} - \Delta R_{\perp})/(\Delta R_{\parallel} + \Delta R_{\perp})$ of 0.19 ± 0.02, which indicates that absorption takes place partly through the nanoantenna [13].

To further investigate the hybrid interaction at the gold-ITO interface, we take advantage of one of the gold pads that was written into the photoresist to optimize the focus before exposure. Such a gold pad is shown in Figure 5, as a SEM picture as well as a picture taken in the home-built microscope. We performed pump probe scans on an area of $20\,\mu\text{m} \times 20\,\mu\text{m}$, both for the slow signal typical for heating of the sample (Figure 5(a)) as well as for the fast pump probe signal. Interestingly, for the heat scan, we observe a clear minimum on the gold pad itself, corresponding to a local heating of the gold surface. For the fast scan (Figure 5(b)), however, the gold pad itself has a clearly positive signal unlike its immediate surroundings. We observe a corona of negative signal up to $2\,\mu$m around the contamination dot, which is even further than the 126 nm hot electron diffusion length that we suggest in [6]. This is partly due to the size of the pump beam (around $2\,\mu$m FWHM), which generates heat and hot electrons in areas around the smaller probe spot.

In conclusion, we have shown ultrafast all-optical control of ITO-nanoantenna hybrids. We identify a picosecond nonlinear response that can be described by an enormous corresponding Kerr-nonlinearity that is a factor of 1475 bigger than for the pure ITO. This huge nonlinearity originates in free carriers being injected from the antenna whose energy generates substantial heat in the surrounding substrate. This is very promising indeed for exploitation in creating nanophotonic switches in other designs and warrants further investigations. Hybrid plasmonic components are of great interest for active control of optical fields and integration of photonic and electronic functionalities. Our antenna-ITO hybrid in particular holds great promise for this since electrically controlled refractive index changes for ITO have already been demonstrated [7].

Acknowledgments

The authors thank Z. Webber and M. A. Bampton for their technical support. O. L. Muskens thanks support from EPSRC through Grant EP/H019669/1.

References

[1] W. L. Barnes, A. Dereux, and T. W. Ebbesen, "Surface plasmon subwavelength optics," *Nature*, vol. 424, no. 6950, pp. 824–830, 2003.

[2] O. L. Muskens, V. Giannini, J. A. Sánchez-Gil, and J. G. Rivas, "Optical scattering resonances of single and coupled dimer plasmonic nanoantennas," *Optics Express*, vol. 15, no. 26, pp. 17736–17746, 2007.

[3] N. Large, M. Abb, J. Aizpurua, and O. L. Muskens, "Photoconductively loaded plasmonic nanoantenna as building block for ultracompact optical switches," *Nano Letters*, vol. 10, no. 5, pp. 1741–1746, 2010.

[4] J. Berthelot, A. Bouhelier, C. Huang et al., "Tuning of an optical dimer nanoantenna by electrically controlling its load impedance," *Nano Letters*, vol. 9, no. 11, pp. 3914–3921, 2009.

[5] F. Huang and J. J. Baumberg, "Actively tuned plasmons on elastomerically driven Au nanoparticle dimers," *Nano Letters*, vol. 10, no. 5, pp. 1787–1792, 2010.

[6] M. Abb, P. Albella, J. Aizpurua, and O. L. Muskens, "All-optical control of a single plasmonic nanoantenna-ITO hybrid," *Nano Letters*, vol. 11, no. 6, pp. 2457–2463, 2011.

[7] E. Feigenbaum, K. Diest, and H. A. Atwater, "Unity-order index change in transparent conducting oxides at visible frequencies," *Nano Letters*, vol. 10, no. 6, pp. 2111–2116, 2010.

[8] A. Arbouet, D. Christofilos, N. del Fatti, F. Vallée, J. R. Huntzinger, and M. Broyer, "Direct measurement of the single-metal-cluster optical absorption," *Physical Review Letters*, vol. 93, Article ID 127401, 2004.

[9] O. L. Muskens, N. del Fatti, F. Vallée, J. R. Huntzinger, and M. Broyer, "Single metal nanoparticle absorption spectroscopy and optical characterization," *Applied Physics Letters*, vol. 88, Article ID 063109, 3 pages, 2006.

[10] H. I. Elim, W. Ji, and F. Zhu, "Carrier concentration dependence of optical Kerr nonlinearity in indium tin oxide films," *Applied Physics B: Lasers and Optics*, vol. 82, no. 3, pp. 439–442, 2006.

[11] S. Link and M. A. El-Sayed, "Spectral properties and relaxation dynamics of surface plasmon electronic oscillations in gold and silver nanodots and nanorods," *Journal of Physical Chemistry B*, vol. 103, no. 40, pp. 8410–8426, 1999.

[12] C. Voisin, D. Christofilos, P. A. Loukakos et al., "Ultrafast electron-electron scattering and energy exchanges in noble-metal nanoparticles," *Physical Review B*, vol. 69, no. 19, Article ID 195416, 2004.

[13] O. L. Muskens, G. Bachelier, N. del Fatti et al., "Quantitative absorption spectroscopy of a single gold nanorod," *Journal of Physical Chemistry C*, vol. 112, no. 24, pp. 8917–8921, 2008.